Published in final edited form as:
J Immunol. 2011 May 1; 186(9): 5356–5366. doi:10.4049/jimmunol.1003794.

A multifunctional element in the mouse *Igκ* locus that specifies repertoire and *Ig* loci subnuclear location[1]

Yougui Xiang[*], **Xiaorong Zhou**[*,‡], **Susannah L. Hewitt**[†], **Jane A. Skok**[†], and **William T. Garrard**[*,2]

[*] Department of Molecular Biology, University of Texas Southwestern Medical Center, 5323 Harry Hines Blvd., Dallas, TX 75390-9148

[†] Department of Pathology, New York School of Medicine, New York, NY 10016

[‡] Department of Microbiology and Immunology, Medical School of Nantong University, 19 Qixiu Road, Nantong, Jiangsu 226001, PR China

Abstract

Non-biased V gene usage for V(D)J joining is essential for providing an optimal immune system, but no *cis*-acting sequence with this function has yet been uncovered. We previously identified Sis, a recombination silencer and heterochromatin targeting element in the Vκ-Jκ intervening sequence of germline *Igκ* transgenes. We now have generated Sis knockout mice in the endogenous locus. Intriguingly, Sis−/− mice exhibit a skewed Igκ repertoire with markedly decreased distal and enhanced proximal Vκ gene usage for primary rearrangement, which is associated with reduced occupancy of IKAROS and CTCF in the Vκ-Jκ intervening sequence in pre-B cells, proteins believed to be responsible for dampening the recombination of nearby Vκ genes and altering higher-order chromatin looping. Furthermore, monoallelic heterochromatin localization is significantly reduced in Sis−/− mice for both *Igκ* in *cis* and *IgH* loci in *trans* in pre-B cells. Because Sis−/− mice still allelically exclude *Igκ* and *IgH* loci and still exhibit *IgL* isotype exclusion, we conclude that stable localization at pericentromeric heterochromatin is neither necessary nor sufficient for the establishment or maintenance of allelic exclusion. Hence, Sis is a novel multifunctional element that specifies both repertoire and heterochromatin localization to *Ig* genes.

Keywords

B cells; V(D)J rearrangement; repertoire; gene regulation; allelic exclusion; heterochromatin; knockout mice; silencers; transcription; 3D FISH

Introduction

During B cell development, the mouse *IgH* and *IgL* loci become activated in a step-wise manner for gene rearrangement. The *IgH* gene rearranges first, by sequential D-J and then by V-(D)J joining, leading to the pro- and pre-B cell stages of development, respectively (1).

[1]This investigation was supported by Grants GM29935 and AI067906 from the National Institutes of Health and Grant I-0823 from the Robert A. Welch Foundation to WTG, and by a Wellcome Trust Project Grant and Grant R01GM086852 from the National Institutes of Health to JAS.

[2]Address correspondence and reprint requests to Dr. William T. Garrard, Department of Molecular Biology, University of Texas Southwestern Medical Center, 5323 Harry Hines Blvd., Dallas, TX 75390-9148. Phone: 214-648-1924. FAX: 214-648-1915. william.garrard@utsouthwestern.edu.

The *Igκ* locus is poised for rearrangement in pre-B cells, and upon appropriate signaling one of the 96 potentially functional Vκ genes is semi-randomly selected for recombination to a Jκ region (2). These events are accompanied by the sequential monoallelic silencing of the allelic partners of the functionally rearranged *IgH* and *IgL* loci (3).

A nearly unlimited antibody repertoire is generated in B lymphocytes by the processes of V(D)J recombination, receptor editing, somatic hypermutation and transcription levels of rearranged genes (4,5). For the immune system to efficiently recognize a broad spectrum of invading pathogens, this diversity in the repertoire is essential. Furthermore, mis-regulated or incorrect repertoire specification can trigger autoimmunity (6,7). Recent evidence has emerged that nuclear organization and locus contraction/decontraction of *Ig* loci contributes to repertoire specification. The mouse *Ig* loci exhibit cell type and differentiation-dependent nuclear reorganization events, which are associated with the regulation of gene rearrangement and gene silencing (e.g., allelic exclusion) (for reviews, 3, 8–10). Results from three-dimensional fluorescence *in situ* hybridization (3D DNA FISH) experiments reveal that the I*gH* and *Igκ* loci exhibit homologous allele pairing, accompanied by contraction and looping of V genes, which juxtaposes them near Dh or Jκ regions in preparation for rearrangement (11–16). Furthermore, reduced contraction of *IgH* loci results in a skewed repertoire, with proximal Vh genes being preferentially utilized (12,17–19), whereas persistent contraction results in greater distal Vh gene rearrangements (20). Decontraction occurs after rearrangement (12), and the allelic partners of the functionally rearranged *IgH* and *Igκ* alleles becoming positioned adjacent to pericentromeric heterochromatin and silenced (21), through transient *IgH-Igκ* monoallelic pairing (20).

Several years ago we discovered a cluster of four DNase I hypersensitive sites within Igκ-locus-chromatin that reside in the intervening sequence between the closest Vκ gene and the Jκ region, which we termed Sis (silencer in the intervening sequence), based on the results of functional assays with reporter gene constructs (22). In subsequent studies we showed that Sis acted as a recombination silencer and could target germline *Igκ* transgenes to pericentromeric heterochromatin in pre-B cells, and that the element was associated with IKAROS (23), a protein that localizes with silenced *Ig* genes at pericentromeric heterochromatin (21,24–26). More recently, Feeney and co-workers have found that Sis also possesses bound CTCF in pre-B cells (27), a protein known to mediate silencing and DNA looping in other systems (28–32).

In view of these intriguing features of Sis, we undertook the present investigation to determine the effects of deleting this element from the endogenous locus on *Igκ* gene dynamics. In our analysis of Sis function, we have focused largely on the pro- and pre-B cell stages of development, which mark the points of activation and silencing of *IgH* and *Igκ* loci, respectively. This approach has led to unexpected novel findings. Significantly, we have found that Sis is required for pericentromeric positioning not only for the *Igκ* loci in *cis*, but also for the *IgH* loci in *trans* in pre-B cells. Furthermore, Sis-deleted alleles exhibit a skewed *Igκ* repertoire, with markedly decreased distal and enhanced proximal Vκ gene usage for rearrangement. Such skewing is correlated with reduction in the occupancy of IKAROS and CTCF in the Vκ-Jκ intervening sequence. We conclude that Sis is a novel multifunctional *cis*-acting element, being a *cis*-acting element that specifies repertoire and both a *cis*- and *trans*-chromosomal subnuclear targeting sequence.

Materials and Methods

Mouse strains

Mice possessing a 3.7 kb deletion of the Sis element in the endogenous *Igκ* locus were generated by standard embryonic stem (ES) cell targeting technology; germline

transmissible mice were bred with Cre recombinase expressing MORE (33) mice to obtain Sis and *neo*^{r} deletion mice (Supplemental Figure S1). Mice bearing a Vκ8Jκ5-knocked-in *Igκ* gene were kindly provided by Martin Weigert (34) of Princeton University. Mice bearing a human Cκ knocked-in gene were kindly provided by Michel C. Nussenzweig of Rockefeller University (4). μ^{+} transgenic mice and Rag1−/− mice were kindly provided by Mark Schlissel of UC Berkeley. All mice were used in accordance with protocols approved by the UT Southwestern Medical Center Institutional Animal Care and Use Committee (IACUC).

Flow cytometry and cell fractionation

Single-cell suspensions were prepared from bone marrow and spleens of 6–14 week old mice as described (35). Generally we pooled bone marrow or splenic cells from 2–3 animals of the same genetic background. Single-cell suspensions were stained with antibodies and analyzed using FACS Calibur with CellQuest software (BD Bioscence, San Diego, CA) or FlowJo software (Tree Star, Ashland, OR). $CD19^{+}c\text{-}Kit^{+}IgM^{-}$ pro-B cells and $CD19^{+}CD25^{+}IgM^{-}$ pre-B cells were sorted on a MoFlo machine (Dako Cytomation, Carpinteria, CA) for 3D-FISH experiments and $B220^{+}IgM^{-}CD43^{+}$ pro-B cells and $B220^{+}IgM^{-}CD43^{-}$ pre-B cells were sorted on a MoFlo machine for other experiments. To assay for RS rearrangement, $B220^{+}Ig\lambda^{+}$ splenic B cells also were sorted on a MoFlo machine. $Ig\kappa^{+}$ cells were isolated by positive selection using biotinylated anti-Igκ Abs (BD Bioscience) and MACS columns (Miltenyi Biotech, Auburn, CA). Antibodies used are as follows: anti-c-Kit-PE (BD Bioscience); anti-CD25-PE (BD Bioscience); anti-CD19-FITC (BD Bioscience); anti-B220-PE (BD Bioscience); anti-mouse-Igκ-PE (BD Bioscience); anti-human-Igκ-FITC (Southern Biotech, Birmingham, AL); anti-IgM-biotin (BD Bioscience); anti-CD43-biotin (BD Bioscience); anti-B220-biotin (BD Bioscience); anti-mouse-Igκ-biotin (BD Bioscience); anti-CD21-FITC (BD Bioscience); anti-IgM-FITC (Southern Biotech); anti-IgD-FITC (Southern Biotech); anti-IgM-APC (Southern Biotech); anti-CD23-APC (Southern Biotech); Streptavidin-APC (Southern Biotech); and Streptavidin-PECy5 (BD Bioscience).

Analysis of Igκ gene rearrangement, RS rearrangement and germline Vκ gene and Jκ region transcription

Genomic DNA was purified from sorted B cell populations as described previously (36). The percentage of unrearranged Igκ germline alleles (κGL) was determined by a real-time PCR assay as described previously (37). Briefly, the forward and reverse primers are complementary to sequences upstream and downstream of Jκ1. κGL levels were normalized to the levels of a β-actin genomic region. The percentage is calculated by dividing the κGL levels in WT or Sis−/− pre-B cells by those in ES cells. For real-time PCR analysis of individual Vκ-Jκ1 rearrangements, forward primers specific to different Vκ exons and a reverse primer complementary to the Jκ1 to Jκ2 intron region were used (primer sequences are listed in Supplemental Table S1). Different Vκ-Jκ1 rearrangements were determined quantitatively by using the power SYBR Green PCR master mix in the 7300 real-time PCR system (Applied Biosystems, Los Angeles, CA). PCR was performed based on manufacturer's protocols and each PCR assay was carried out in duplicate or triplicate. Relative rearrangements were calculated using the ΔC_t method according to the manufacturer's instructions and normalized to an β-actin genomic region. For Igκ repertoire analysis, the VκD primer (38) and a primer in the Jκ1 intron were used to amplify Vκ-Jκ1 rearrangements, or the VκD primer and the Jκ5R primer downstream of Jκ5 were used to amplify Vκ-Jκ5 rearrangements; resulting PCR products were gel purified and subcloned into the PGEM-T vector (Promega, San Luis Obispo, CA). Determined sequences of Vκ genes in each clone were identified by the IgBlast program (NCBI, Bethesda, MD). N- and P-nucleotides were determined as described elsewhere (39).

To assay for RS rearrangement, $B220^{+}Ig\lambda^{+}$ B cells were sorted from splenocytes, and genomic DNA was purified. Real-time PCR then was performed with the VκD and the RS101 primer (40) (Supplemental Table S1). Relative rearrangements were calculated using the ΔC_t method according to the manufacturer's instructions and normalized to a β-actin genomic region.

To examine *Igκ* gene germline transcription, total RNA was extracted from 1×10^6 MoFlo sorted pre-B cells using TRIzol reagent (Invitrogen, Carlsbad, CA). Then RNA was treated with DNase I (Invitrogen) and was reverse transcribed into cDNA with iScript cDNA Synthesis Kit (Bio-Rad laboratories, Richmond, CA). For real-time PCR analysis of individual Vκ gene's germline transcripts, forward primers specific to different Vκ gene exons and a reverse primer complementary to the downstream RSS region were used (Supplemental Table S1). For analysis of transcripts arising from the 5′ germline promoter upstream of the Jκ1 region, a forward 5′GT-f primer annealing immediately downstream of the promoter region and a reverse Cκ-r primer annealing in Cκ exon were used in real time PCR assays (Supplemental Table S1). Transcript levels were calculated using the ΔC_t method according to the manufacturer's instructions and normalized to the cDNA levels of the mouse β-actin gene.

FISH and 3D imaging

Probes for 3D FISH were prepared from bacterial artificial chromosomes (BACs). RP23-119K14, RP23-26A6, and RP24-387E13 correspond to the 5′, middle, and Cκ region of the *Igκ* locus, respectively. CT7-526A21 and RP23-451B13 are BACs corresponding to the 5′ Vh region and Ch region of the *IgH* locus. The γ-satellite probe was gel isolated from pγSat after *Not*I/*Sal*I digestion (41). In order to make probes for each slide, 1 μg BAC DNA samples were labeled by nick translation with ChromaTide Alexa Fluor 488-5-dUTP, ChromaTide Alexa Fluor 594-5-dUTP (Molecular Probes, Invitrogen, Carlsbad, CA) or dUTP-indodicarbocyanine (Cy5, GE Healthcare, Piscataway, NJ), and precipitated with 1 μg mouse Cot-1 DNA (Invitrogen) plus 1 μg mouse Hybloc DNA (Applied Genetics Laboratories). Cot-1 DNA and mouse hybloc DNA were not used for making the γ-satellite probe. Z stacks with sections separated by 0.3 μm were analyzed by confocal microscopy using a Leica SP5 instrument and distances were measured using a pluggin of ImageJ software (42). Hybridization conditions were as described previously (24). Briefly, sorted cells were washed three times in PBS and then were fixed on poly-L-lysine-coated slides for 30 min with fixation permeabilization buffer (20 mM KH_2PO_4, 130 mM NaCl, 20 mM KCl, 10 mM EGTA, 20 mM $MgCl_2$, O.1% [v/v] Triton X-100, and 0.5% [v/v] glutaraldehyde [Sigma Aldrich, St. Louis, MO, grade 1, 70% aqueous]), and washed three times in PBS and twice (15 min/wash) with sodium borohydride solution (1 mg/ml prepared freshly in water). The samples were sequentially incubated with PBS with 5% goat serum/5% FCS for 30 min, for 1 hr with RNase (100 μg/ml in PBS), washed in PBS, and the chromosomal DNA denatured by placing the coverslips in 1 M NaOH for 2 min and rinsing immediately in ice-cold PBS prior to applying DNA probes. Hybridization was performed overnight at 37°C in humidified chambers. Slides were washed in the dark in 2x SSC for 30 min at 37oC, 2x SSC for 30 min at room temperature and 1x SSC for 30 min at room temperature and then were mounted in ProLong Gold (Invitrogen) mixed with 1.5 μg/ml DAPI.

ChIP

In order to obtain adequate amounts of pre-B cells for Ikaros ChIP experiments, which required about 1×10^8 cells, we bred μ^+ transgenic mice with Rag1−/− mice (kindly provided by Mark Schlissel), and with Sis−/− mice, to establish pre-B cell animal models with the genotypes Rag1−/−, Sis+/+, μ^+ transgenic and Rag1−/−, Sis−/−, μ^+ transgenic in the F2 generations (43,44). Ikaros ChIP using antibodies kindly provided by Stephen Smale, (UC

Los Angeles, CA) were performed as described elsewhere (23). For CTCF, H3-Ac and H3K4me3 ChIP, about 2×10^6 sorted pre-B ($B220^+IgM^-CD43^-$) cells or $CD19^+$ pre-B cells from Rag1−/−, μ^+transgenic animal models were used for each ChIP experiment. ChIP experiments were conducted according to the protocol of Millipore. Rabbit anti-CTCF antibodies (Millipore, 07-729), Rabbit anti-H3-Ac antibodies (Millipore, 06-599), and Rabbit anti-H3K4me3 antibodies (Millipore, 07-473) were used for ChIP and Normal rabbit IgG (Invitrogen) were used as controls. Real-time PCR was performed and quantitated using the 7300 Real Time PCR System (Applied Biosystems) with SYBR green as described above and enrichment of target regions in ChIP was normalized to an α-actin gene sequence (primer sequences are listed in the Supplemental Table S1).

Results

Sis−/− mice exhibit normal surface Ig expression and B cell development in spleen and bone marrow

To examine the function of Sis in the endogenous *Igκ* locus, we generated germline transmissible mice with a targeted 3.7 kb deletion of Sis, leaving only a single loxP site in its place, through standard ES cell targeting technology. Various stages of the targeting and Sis deletion were confirmed by Southern blotting (Supplemental Fig. S1). We found that Sis−/− mice exhibited no significant differences in bone marrow and spleen cell numbers or spleen weight compared to those of their WT littermates or age-matched WT mice. [bone marrow cell numbers (2 femurs and 2 tibias): 50.7±3.8 vs 49.8±6.3 × 10^6, n=9, *P*=0.74 Student's *t* test; spleen cell numbers: 126.5±21.8 vs 122.8±19.8 × 10^6, n=6, *P*=0.77 Student's *t* test; or spleen weight: 102±12.4 vs 93.7±15.0 mg, n=10, *P*=0.19 Student's *t* test]. Furthermore, Sis −/− mice exhibited similar levels of $Ig\kappa^+$ B cells in spleen compared with WT mice (Fig. 1*A*; 52.6±2.9% versus 53.3±5.7%, as percentages of $Ig\kappa^+$ B cells among total lymphocytes, n=6, *P*=0.8 Student's *t* test). Moreover, the percentages of $Ig\lambda^+$ B cells were nearly identical between Sis−/− and WT mice in spleen (Fig. 1*A*; 2.4±0.5% versus 2.3±0.4%, n=6, *P*=0.65, Student's *t* test). We further investigated the effect of Sis deletion on the development of B cell subpopulations in spleen by FACS, and found that they were all normal relative to those of WT mice, including the percentages of transitional T1 B cells (Fig. 1*B*, $IgM^{hi}IgD^{lo}$, 8.7±2.1% vs 9.8±2.4%, n=6, *P*=0.45 Student's *t* test), transitional T2 B cells (Fig. 1*B*, $IgM^{hi}IgD^{hi}$, 10.3±1.9% vs 12.2±2.8%, n=6, *P*=0.21 Student's *t* test), follicular mature B cells (Fig. 1*B*, $IgM^{int}IgD^{hi}$, 25.6±2.3% vs 26±2.0%, n=6, *P*=0.74 Student's *t* test), and marginal zone B cells (Fig. 1*B*, $CD21^+CD23^{lo}$, 5.0±1.2% vs 4.7±0.8%, n=8, *P*=0.57 Student's *t* test).

Likewise, the percentages of $Ig\kappa^+$ cells in bone marrow were not significantly different between Sis−/− and WT mice (Fig. 1*C*, 20.5±1.7% vs 20.6±2.3 %, n=6, *P*=0.94 Student's *t* test). We also observed similar levels of $Ig\lambda^+$ cells in bone marrow in Sis−/− mice as compared to those of WT (Fig. 1*C*, 1.4±0.6% vs 1.6±0.6%, n=8, *P*=0.38 Student's *t* test). Finally, we evaluated the pro-B, pre-B and IgM^+ cell compartments in bone marrow from Sis−/− and WT mice by FACS, and found no significant differences in the percentages of $B220^+c\text{-}kit^+$ pro-B cells (Fig. 1*D*, 2.5±0.3% vs 2.4±0.3%, n=9, *P*=0.52 Student's *t* test), $B220^+CD25^+$ pre-B cells (Fig. 1*D*, 13.2±3.4% vs 12±2.9%, n=9, *P*=0.44 Student's *t* test), and bone marrow $B220^+IgM^+$ B cells (Fig. 1*D*, 19±5% vs 21.4±2%, n=7, *P*=0.27 Student's *t* test). We conclude that deletion of Sis causes no significant defects in B cell development or in cell surface Ig expression in spleen and bone marrow cells.

Sis specifies pericentromeric heterochromatin positioning of Igκ loci in cis and IgH loci in trans in pre-B cells

During the pro- to pre-B cellular transition, *Igκ* and *IgH* loci become repositioned monoallelically into pericentromeric heterochromatin; furthermore, this monoallelic deposition of *IgH* alleles into heterochromatin requires their transient close physical association with *Igκ* alleles, which is dependent on the *Igκ* gene's 3′ enhancer (12,20,26). Because our previous studies have demonstrated that Sis can specify pericentromeric heterochromatin positioning to germline mouse *Igκ* transgenes in pre-B cells (23), we wanted to determine whether Sis would be the essential element for this process to occur in the endogenous locus. In addition, we wished to address how deletion of Sis may affect the interchromosomal association between one *Igκ* allele and one *IgH* allele and their colocalization to heterochromatin. For these purposes we performed three-color 3D DNA FISH, using a 5′ *Igκ* probe shown as red, a 5′ *IgH* probe depicted as green, and a γ-satellite probe represented as blue, on FACS-isolated pro- and pre-B cells from the bone marrow of WT and Sis−/− mice. Fig. 2*A* and *B* shows representative confocal optical sections of probe hybridization patterns for single nuclei of these samples. The pair of sections presented from single cells in the upper and lower subpanels permit visualization of the two *Igκ* and the two *IgH* alleles and assessment of their possible localization with respect to heterochromatin. Histograms reflecting the percentages of heterochromatin localization are shown in Fig. 2*C*. In pro-B cells we found that between 22% to 27% of *IgH* and *Igκ* alleles each exhibit monoallelic heterochromatin localization for both WT and Sis−/− samples. By contrast, in pre-B cells of WT mice, about 58% and 71% of *IgH* and *Igκ* alleles exhibit monoallelic heterochromatin localization, respectively, whereas the respective corresponding pre-B cell samples from Sis−/− mice only exhibit about 27% and 35% monoallelic heterochromatin localization (Fig. 2*C*). Analysis of these pre-B cell data using Fisher's exact test reveals that the nuclear distributions are significantly different between WT and Sis−/− samples ($P<0.01$). In addition, these results are highly reproducible in several repeat experiments (Supplemental Table S2*A,B,C*). These observations allow us to conclude that Sis plays a major role in targeting of both *Igκ* and *IgH* loci to heterochromatin domains in pre-B cells. We also note that there is a small but statistically significant increase in biallelic localization in heterochromatin of both *Igκ* and *IgH* loci in Sis−/− pre-B cells that could be judged only when we repeated these experiments three to four times so that from 276 to 440 samples' measurements could be pooled ($P<0.04$) (Supplemental Table S2*D*). Thus, Sis also appears to play a modest role in counteracting biallelic localization in heterochromatin. Previous studies have also shown that one *IgH* allele and one *Igκ* allele exhibit significant interchromosomal pairing in pre-B cells, which is operationally defined as *Igκ* alleles that are <0.5μm away from *IgH* alleles (20). Because we used three-color 3D DNA FISH we were also able to quantitate such pairing in these same specimens. As shown in the histograms of Fig. 2*D*, like WT alleles, about 20% of Sis- alleles are <0.5μm away from *IgH* alleles in pre-B cells. Analysis of these data using Fisher's exact test reveals that the frequency of association is not significantly different between WT and Sis−/− samples ($P<0.68$) (Supplemental Table S2*E*). We conclude that Sis is both a *cis*- and *trans*-chromosomal subnuclear targeting sequence for monoallelic pericentromeric heterochromatin localization of *Igκ* and *IgH* alleles in pre-B cells, but that Sis is not required for the monoallelic pairing of *Igκ* and *IgH* alleles.

Sis−/− mice exhibit normal levels of allelic exclusion

The above results reveal that Sis is responsible in *cis* and *trans* for monoallelically targeting the native *Igκ* and *IgH* loci to a repressive heterochromatin environment and our previously published results demonstrated that Sis acts as a recombination silencer when present in germline mouse *Igκ* transgenes (23). These intriguing observations led us to hypothesize that Sis may specify allelic exclusion, and that Sis−/− alleles may exhibit allelic inclusion in *cis*

for *Igκ* and possibly in *trans* for *IgH* loci. To stepwise test these possibilities, we first bred Sis−/− mice with mice carrying a human Cκ knockin allele (4), and found by FACS analysis that heterozygotes exhibited very similar levels of near exclusive usage of either the mouse or the human Cκ exons, with very few double positive expressing cells, regardless of the presence or absence of Sis, in both splenic and bone marrow tissues (Fig. 3*A*,*B*). We next evaluated *IgL* isotype inclusion of *Igκ* and *Igλ* loci in WT control and Sis−/− mice splenic B cells by FACS analysis. As shown in Fig. 3*C*, we observed very few double isotype positive cells in both WT and Sis−/− mice samples. Finally, to test whether *IgH* loci still exhibit allelic exclusion in Sis−/− mice, we generated $IgM^{a/b}$, Sis+/+ and $IgM^{a/b}$, Sis−/− mice after selective breeding of 129/SvTac mice lines with C57BL/6 mice for FACS analysis of *IgH* allotypic usage. As shown in Fig. 3*D*, we found very few double positive $IgM^{a/b}$ producers in both the WT control and Sis−/− mice bone marrow cells. We conclude that within the context of the sensitivity of these assays and the combined results, Sis does not interfere significantly with allele usage and is neither necessary nor sufficient to specify allelic exclusion in *cis* for *Igκ* or in *trans* for *IgH* loci.

Sis−/− mice exhibit a skewed Igκ gene repertoire with markedly decreased distal and enhanced proximal Vκ gene usage

The mouse *Igκ* locus possesses 96 potentially functional Vκ genes and 65 of these genes are in the reverse transcriptional orientation with respect to the Jκ-Cκ region (2). Rearrangement of forward orientation Vκ genes will result in deletion of Sis from the WT locus, whereas rearrangement of reverse orientation Vκ genes from the WT locus will result in repositioning of Sis upstream in the locus by inversion. The closest Vκ gene in the reverse orientation is Vκ19-13, which resides 265 kb from Jκ1, while the furthest Vκ gene in the reverse orientation is Vκ9-126, which resides 2,780 kb from Jκ1 (2). In addition, repeated rearrangement events occur in the locus due to receptor editing. Primary rearrangement events preferentially use Jκ1 (45,46), reserving the downstream Jκ regions for receptor editing (4,34,40,47,48; for review, see ref. 49). Considering these issues we have looked more closely at the effect of Sis on the rearrangement of forward and reverse orientation Vκ genes Jκ1, and for their repeated rearrangement likely exemplified by Vκ-Jκ5 rearrangements.

We previously demonstrated that Sis acts as a silencer for the rearrangement of forward orientation Vκ genes located at distances at least 190 kb away from Jκ1 when present in ectopically integrated germline mouse *Igκ* transgenes (23). To investigate whether deletion of Sis would also alter the pattern of primary Vκ gene usage in the native locus we first used real-time PCR to quantitate relative Vκ-Jκ1 gene rearrangement levels for fourteen different Vκ genes located in segments of the locus spanning 3 Mb in either forward or reverse orientations (Fig. 4*A*). In IgM^- pre-B cells, and in κ^+ bone marrow and splenic cells, the individual Vκ gene rearrangement levels differed markedly for Sis deleted alleles from those of WT (Fig. 4*B*–*D*). However, total rearrangement levels for Sis deleted alleles as assayed with a degenerate Vκ gene primer (VκD) were similar to those of WT (Fig. 4*B*–*D*), as were rearrangement levels for members of the abundant centrally located reverse orientation Vκ4 gene family, as assayed for using a degenerate Vκ4D primer (data not shown). Interestingly, the forward orientation Vκ21 genes closest to the Jκ region were 4-fold preferred for Vκ-Jκ joining, and those further away, such as Vκ2,9,24,32 family members, showed a 3-fold reduction in rearrangement levels relative to those of WT (Fig. 4*B*–*D*). The fairly closely positioned reverse orientation Vκ19-15 gene also exhibited a significant increase in usage in Sis−/− splenic and pre-B cells (Fig. 4*B*,*D*).

To validate these results by an independent approach, we cloned and sequenced VκD-Jκ1 PCR amplification products from the DNA of WT and Sis−/− pre-B cells. Consistent with the real-time PCR results, we found that the usage of the most proximal 32 Vκ genes was

increased about 3-fold in Sis−/− samples relative to those of WT, including members in both forward and reverse orientations in the Vκ13-32 group, while the usage of the most distal Vκ118-140 group forward orientation genes that were used in WT samples were decreased about 5-fold in Sis−/− samples (Fig. 4*E*). Most of the Vκ genes in the middle of the locus in either orientation exhibited normal usage with the exception the reverse orientation Vκ49 to Vκ70 gene cluster, which exhibited reduced usage in Sis−/− samples (Fig. 4*E*). This skewed repertoire is also reflected at the level of RNA expression, as proximal Vκ gene transcripts were increased about 5–8 fold in splenic tissue from Sis−/− mice relative to those of WT as revealed by real-time RT-PCR assays with isolated RNA samples (data not shown). As expected, the percentages of N and P nucleotides and in-frame recombination junctions were nearly identical between WT and Sis−/− pre-B cell samples (data not shown), indicating that Vκ-Jκ recombination products are functional in Sis−/− mice, and that the timing of Vκ-Jκ rearrangement is not affected by Sis deletion. In conclusion, while the total Vκ-Jκ rearrangement level is not affected by deletion of Sis, the pattern of primary Vκ gene usage is markedly altered. The results suggest that Sis is a negative regulator of the usage of proximal Vκ genes located at distances up to 650 kb away from Jκ1 regardless of their orientation, and a positive regulator of distal Vκ genes located at distances from 3,166 to 2,617 kb away from Jκ1 regardless of their orientation.

Finally, to address whether the presence of Sis might have an impact on repeated rearrangements in the locus during receptor editing, we cloned and sequenced VκD-Jκ5 PCR amplification products from the DNA of WT and Sis−/− pre-B cells. The most dramatic difference between Vκ gene usage in primary and edited rearrangements is the pattern seen in the distal upstream Vκ118-140 group, which included Sis-independent usage of Vκ gene members in both orientations (compare Fig. 4*E* with Fig. 4*F*). Here, we hypothesize that these rearrangements to Jκ5 are occurring on WT alleles that have already deleted Sis due to earlier deletional rearrangements. Finally, we still observe Sis dependent inhibition of rearrangements for the Vκ13-32 group for Jκ5 rearrangements, which includes usage of Vκ gene members in both orientations, and for the forward orientation Vκ1-12 group (compare Fig. 4*E* with Fig. 4*F*). We interpret these results to indicate that after inversional primary rearrangements and movement of Sis upstream at the very least 265 kb away from Jκ1 that Sis is inhibitory to the repeated rearrangement process when it is present within approximately 650 kb from the Vκ gene selected for rearrangement, regardless of the position of the Vκ gene in the locus. Presumably, primary rearrangement events leading to inversion and placement of Sis upstream in the locus but still in proximity with the Vκ1-32 gene groups leads to these results.

Jκ region usage, Igκ gene germline levels and RS recombination appear normal in B cell populations from Sis−/− mice

Our above results reveal that primary Vκ gene usage is skewed in Sis−/− B cells, but that overall primary rearrangement levels for Sis deleted alleles as assayed with a degenerate Vκ gene primer (VκD) to Jκ1 were similar to those of WT (Fig. 4*B–D*). To further address other aspects of primary and edited rearrangement events we performed additional PCR assays. We examined the relative usage of Jκ1-5 regions in splenic B cells using a degenerate VκD primer and the Mar35 primer (Fig. 5*A*,*B*,*C*). We found that each of the four functional Jκ regions were used in Vκ-Jκ joining in Sis−/− mice at equivalent levels compared to those of WT controls (Fig. 5*B*,*C*). To determine whether total rearrangement levels might be more extensive in Sis−/− mice as compared to WT, we used a real-time PCR assay to evaluate the germline levels of *Igκ* sequences in pro-B, pre-B, and κ^+ bone marrow and splenic cells from Sis−/− mice and corresponding samples from WT controls (Fig. 5*D*). We found that the germline levels of *Igκ* sequences between Sis−/− mice and WT counterparts in each of these samples were almost identical, which indicates that the total Vκ-Jκ rearrangement does

not increase after deletion of Sis from the endogenous locus (Fig. 5*D*). We also confirmed that the percentage of *Igκ* germline sequences in bone marrow were at the same level as in splenic Igκ$^+$ cells in both WT and Sis−/− mice samples by using a Southern blotting assay (data not shown). In addition, we observed very similar levels of gene rearrangement between WT and Sis−/− alleles after breeding to achieve heterozygotic genetic backgrounds in which one *Igκ* allele was pre-rearranged in the Vκ8-Jκ5 knockin mouse line (34) (Fig. 5*E*). We also used a real-time PCR assay to evaluate rearrangement to the RS element in λ-producing splenic B cells from WT and Sis−/− mice using the degenerate VκD primer and primer RS101 (Fig. 5*A*). This assay revealed that Vκ-RS rearrangement was about 1.2-fold higher in Sis−/− mice samples (Fig. 5*F*). Finally, we found that *Igκ* gene rearrangement was undetectable in sorted T cells from WT and Sis−/− mice, and similarly very low in sorted pro-B cells (Supplemental Fig. S2). To summarize these results, we conclude that within the context of the sensitivity of these assays and the combined results, Sis does not interfere significantly with allele or Jκ region usage but may modestly inhibit Vκ-RS rearrangement leading to increased editing in Sis−/− B cells, possibly because of the skewed Vκ gene repertoire.

Investigation of mechanisms possibly responsible for alterations of the Igκ gene repertoire caused by Sis

Previous studies have linked several histone post-translational modifications to the activation of immunoglobulin genes in preparation for their undergoing V(D)J joining (for reviews, see refs. 50,51). Furthermore, two hallmark modifications for locus activation in pre-B cells are acetylation of histone H3 (H3-Ac) and trimethylation of lysine 4 of histone H3 (H3K4me3) in the Jκ region (52). Therefore, to characterize the epigenetic chromosomal state of the Igκ locus in Sis−/− mice pre-B cells relative to WT controls, we performed ChIP experiments with anti-H3-Ac and anti-H3K4me3 antibodies and utilized real-time RT-PCR to quantitate the results. Because Vκ usage was skewed in Sis−/− mice, we also assayed the levels of these histone marks in several Vκ genes besides Jκ1. In agreement with previously published results (52), we found strikingly high levels of these modifications in the Jκ1 region in WT mice samples, and although very high, these levels were reduced 2- to 3-fold in Sis−/− samples (Fig. 6*A*,*B*). Among the Vκ genes assayed, the most significant enrichments were observed for the far upstream Vκ2-139 gene (Fig. 6*A*,*B*), which notably showed a 2-fold lower level of the H3K4me3 positive epigenetic mark in Sis−/− samples (Fig. 6*B*); this reduction correlates with the reduced usage of this Vκ gene in primary rearrangement events (Fig. 4*B*–*D*).

Germline transcription of the Igκ locus in pre-B cells has long been thought to increase locus accessibility to the recombinase apparatus and has been correlated with the process of Vκ-Jκ joining (38,53). We therefore assayed for germline transcripts in pre-B cells from WT and Sis−/− mice, arising from the 5′ germline promoter upstream of Jκ1 (54), and for numerous other germline transcripts arising from different specific Vκ genes. As shown in Fig. 6*C*, we observed a general 1.5- to 3-fold increase in the steady-state levels of germline transcripts derived from both proximal and distal regions in the locus that does not correlate with the patterns observed for Vκ gene usage. This observed overall increase in germline transcription throughout the locus may be a consequence or a cause of reduced pericentromeric heterochromatin localization. These results are consistent with our previously published results using artificial reporter gene constructs that Sis acts as a pre-B cell-specific transcriptional silencer (22).

Sis is known to bind both IKAROS and CTCF in pre-B cells (23,27), proteins previously documented to silence sequences nearby their binding sites (24–26,28–32). Hence, the preferential rearrangement of proximal Vκ genes in Sis−/− mice might be explained by the hypothesis that these Sis-associated-proteins reduce the accessibility of proximal Vκ genes

to the recombination machinery. In order to specifically address the effects of Sis deletion on the recruitment of these proteins, we sheared cross-linked chromatin from pre-B cells of Sis+/+ and Sis−/− mice to fragments 1- to 2-kb long so that a 3′ adjacent primer pair could be used to detect sequences common to both Sis−/− and WT alleles after ChIP by real-time PCR assays (Fig. 6*D*, top). After immunoprecipitation with anti-IKAROS or anti-CTCF antibodies, we found that the assayed sequences in Sis+ alleles were significantly enriched relative to their sequence abundancies in input chromatin DNA samples (Fig. 6*D*). By contrast, immunoprecipitated samples from Sis-alleles exhibited no enrichment in the sequences assayed for over their abundance in total input chromatin (Fig. 6*D*). We conclude that Sis plays an essential role in *cis* for the recruitment of both IKAROS and CTCF to the *Igκ* locus V-J intervening sequence in pre-B cells.

Sis−/− mice still exhibit normal Igκ locus contraction and looping in pre-B cells

Previous studies employing 3D FISH have revealed that at the onset of V(D)J rearrangement of *IgH* and *Igκ* loci, the corresponding alleles exhibit contraction and looping (10,12). Furthermore, when *IgH* locus contraction is reduced in several genetically engineered mouse models, only proximal Vh genes are favored for rearrangement, which results in a skewed repertoire (12,17–19). By analogy, we hypothesized that contraction and looping may be reduced in *Igκ* loci of Sis−/− mice pre-B cells and may account for the preferential usage of proximal Vκ genes. To test this possibility, we performed two-color 3D FISH experiments using *Igκ* BAC probes corresponding to 5′ and 3′ locations in the locus and quantitated the extent of contraction of the locus in pre-B cell samples from WT and Sis−/− mice. However, as shown in Fig. 7, both WT and Sis−/− *Igκ* alleles exhibit an essentially identical extent of contraction. In addition, when we used three-color 3-D FISH to examine looping in *Igκ* loci, we also observed very similar images between WT and Sis−/− pre-B cell samples (data not shown). Therefore, we conclude that within the limits of sensitivity of these assays, Sis plays no obvious role in conferring interactions between distal and proximal sequences in the *Igκ* locus in pre-B cells that contribute to contraction and looping.

Discussion

In an earlier study we demonstrated that Sis could target 225-kb germline *Igκ* transgenes to pericentromeric heterochromatin in pre-B cells (23). In the present investigation our results reveal that the element is largely responsible for monoallelically targeting of entire 3.2-Mb endogenous loci to such heterochromatin domains. This deserves special appreciation considering the fact that Sis only represents about 0.12% of the total sequences by length in the locus. Even more remarkable, Sis is also largely responsible for targeting *IgH* loci to such heterochromatin domains. Previous studies have shown that *IgH* and *Igκ* loci associate at pericentromeric heterochromatin in pre-B cells, and that this inter-chromosomal interaction requires the *Igκ* 3′ enhancer (20). We have found that *IgH* and *Igκ* loci still interact in pre-B cell nuclei from Sis−/− mice, but like *Igκ* alleles, *IgH* alleles no longer become localized to heterochromatin. Therefore, we conclude that Sis is required *trans*-chromosomally for localization of *IgH* to pericentromeric heterochromatin by a piggy-back mechanism.

In Sis−/− pre-B cells we observed a significant decrease in the frequency with which *IgH* and *Igκ* were positioned at pericentromeric heterochromatin. However, despite their euchromatic location, allelic and isotypic exclusion remain intact. In this context homologous pairing may be the signal for initiating allelic exclusion in *Ig* loci (10,16), just as pairing between maternal and paternal X-chromosomes is known to be linked to the process of X-inactivation in developing female cells (42,55,56). We already know that RAG-mediated pairing of homologues triggers repositioning of one *Igκ* allele to pericentromeric heterochromatin and that normally in pre-B cells repositioning of *Igκ* occurs

in an apparently stable manner: approximately 70% of cells have one allele repositioned at pericentromeric regions. In contrast, in the absence of RAG, pairing and association of *Igκ* are significantly reduced. Interestingly, in the absence of Sis, homologous pairing of *Ig* alleles remained unaffected (Supplemental Table S2*H,I*), while in contrast, association with pericentromeric heterochromatin was significantly reduced. Pairing of *Igκ* homologues and repositioning of one allele to pericentromeric heterochromatin could still occur, but stable localization is likely antagonized by the elevated levels of *Igκ* germline transcription that are found in Sis−/− pre-B cells. In this context transient repositioning of *Igκ* with pericentromeric heterochromatin is likely to be associated with a transient reduction in accessibility. However, continued homologous pairing and shuttling of alleles backwards and forwards between euchromatin and heterochromatin could still be sufficient to impose allelic exclusion.

While previous studies have identified *trans*-acting factors that modulate the *Igκ* gene repertoire (5,7), Sis is the first example of a *cis*-acting sequence that is required for repertoire specification. In primary rearrangement events we observe preferential usage of Jκ-proximal Vκ genes, with severe dampening of distal Vκ gene usage. This skewing of Vκ gene usage seen in B cells is not a result of clonal selection because similar alterations in repertoire are observed in IgM-minus pre-B cells in bone marrow. The increase in rearrangement of proximal Vκ genes upon Sis deletion is not a consequence of physically bringing these genes closer to Jκ gene segments. The foreshortening of the 20 kb Vκ-Jκ intervening sequence is small due to the deletion of the 3.7 kb Sis sequence, whereas Vκ genes even up to 650 kb upstream of this deletion exhibit markedly increased usage in recombination, regardless of their orientation. Sis also appears to play a positive role for the primary rearrangement of the far upstream Vκ genes, whose rearrangement is severely dampened in Sis−/− mice. Because genetically engineered animal models that result in preferential rearrangement of Dh-proximal Vh genes exhibit less contraction and looping in pro-B cells (12,17–19), we hypothesized that Sis may play a role in *Igκ* locus contraction and looping in pre-B cells. However, at the limited level of resolution of our 3D FISH experiments, we could find no evidence to support the notion that Sis plays a role in locus contraction or looping. To improve resolution for the detection of alterations in *Igκ* locus higher order chromosome structures caused by deletion of Sis we have performed several capturing chromosome conformation (4C) experiments (57,58), but we have not been able to obtain reproducible results utilizing such techniques, possibly because of the potential dynamic nature of various synapses in the locus in pre-B cells (our unpublished observations). In other studies it has been demonstrated that germline transcription in the *Igκ* locus is required for Vκ-Jκ joining (53). However, when we assayed for germline transcripts in pre-B cells from Sis−/− mice, we observed a general 1.5- to 3-fold increase in the steady-state levels of these components derived from both proximal and distal regions in the locus that did not correlate with the patterns observed for Vκ gene usage. We also assayed for the epigenetic positive histone marks that have been reported to be heavily enriched in the Jκ region in pre-B cells (52). While acetylation levels did not correlate with altered Vκ gene usage in Sis−/− mice pre-B cells, we did observe a 2-fold reduction in H3K4me3 levels in the far upstream Vκ2 gene, which does correlate with its reduced usage in primary rearrangements.

We previously demonstrated that Sis acts as a silencer for the rearrangement of forward orientation Vκ genes located at distances at least 190 kb away from Jκ1 when present in ectopically integrated germline mouse *Igκ* transgenes (23). We found that deletion of Sis from such transgenes resulted in a 5- to 7-fold increase in Vκ gene rearrangement in bone marrow (23). Our current results are extremely consistent with these earlier findings and provide direct evidence for such silencer activity of nearby Vκ genes in the native locus. The silencer activity seems to progressively dissipate the further the Vκ gene is away from Sis

and is no longer effective when Vκ genes reach distances greater than 650 kb away from Sis. In addition, we have evidence from Vκ gene usage in presumptive edited rearrangements that the recombination silencing activity of Sis is a function of its distance from the Vκ gene to be used for rearrangement and not the distance of Sis from Jκ1. The primary function of Sis in repertoire specification may be to dampen the recombination frequencies of Vκ genes very close to the Jκ regions, so as to even out the usage of more distal Vκ genes spanning the entire 3 Mb locus, as well as to provide a complementary enhancing effect on distal Vκ gene usage.

In conclusion, our results reveal that Sis is a multifunctional *cis*-acting element, which is involved in subnuclear targeting of germline *Ig* sequences both in *cis* and in *trans*, and in specification of the repertoire in rearranging alleles. We hypothesize that these functions should be separable, as the element itself possesses four DNase I hypersensitive sites in chromatin and is associated with at least two different DNA binding proteins. IKAROS is known to have a DNA binding domain and a protein interaction domain, and the protein forms homo- and hetero-dimers with interacting partners through its protein interaction domain (59). IKAROS is not only associated with Sis, but it also specifically associated with γ-satellite DNA sequences, which also are localized in pericentromeric heterochromatin (60). Hence, IKAROS homo-dimer formation between complexes bound to Sis and γ-satellite could be responsible for pericentromeric heterochromatin targeting. CTCF is an insulator binding protein associated with silencing the activity of adjacent enhancers, and it also can play roles in DNA looping and association with cohesin (28–32,61–65). We propose that the known association of Sis with CTCF and cohesin (27) may be involved in the local silencing of proximal Vκ genes to dampen their usage in recombination, and in alterations in higher-order chromatin looping enhancing distal Vκ gene usage in recombination. Site-directed mutagenesis experiments in the future may offer support to these proposals.

Supplementary Material

Refer to Web version on PubMed Central for supplementary material.

Acknowledgments

We are indebted to Stephen Smale of the University of California at Los Angeles for his generous gift of anti-Ikaros antisera and advice in cross-linking, to Niall Dillon for the gift of the pγSat plasmid, to Jose Cabrera for graphics, and to Michel Nussenzeig, Mark Schlissel, Michelle Tallquist, and Martin Weigert for providing mouse lines.

Abbreviation

Sis	Silencer in the intervening sequence
3D FISH	3D fluorescent *in situ* hybridization
ChIP	Chromatin immunoprecipitation

References

1. Yancopoulos GD, Alt FW. Developmental controlled and tissue-specific expression of unrearranged VH gene segments. Cell. 1985; 40:271–281. [PubMed: 2578321]
2. Brekke KM, Garrard WT. Assembly and analysis of the mouse immunoglobulin kappa gene sequence. Immunogenetics. 2004; 56:490–505. [PubMed: 15378297]
3. Vettermann C, Schlissel MS. Allelic exclusion of immunoglobulin genes: models and mechanisims. Immunol Rev. 2010; 237:22–42. [PubMed: 20727027]

4. Casellas R, Shih TAY, Kleinewietfeld M, Jankovic M, Nemazee D, Rajewsky K, Nussenzweig MC. Contribution of receptor editing to the antibody repertoire. Science. 2001; 291:1541–1544. [PubMed: 11222858]
5. Casellas R, Jankovic M, Meyer G, Gazumyan A, Luo Y, Roeder RG, Nussenzweig MC. OcaB is required for normal transcription and V(D)J recombination in a subset of immunoglobulin κ genes. Cell. 2002; 110:575–585. [PubMed: 12230975]
6. Jankovic M, Nussenweig MC. OcaB regulates transitional B cell selection. Internat Immunol. 2003; 15:1099–1104.
7. Ishida D, Su L, Tamura A, Katayama Y, Kawai Y, Wang SF, Taniwaki M, Hamazaki Y, Hattori M, Minato N. Rap1 signal controls B cell receptor repertoire and generation of self-reactive B1a cells. Immunity. 2006; 24:417–427. [PubMed: 16618600]
8. Cedar H, Bergman Y. Choreography of Ig allelic exclusion. Curr Opin Immunol. 2008; 20:308–317. [PubMed: 18400481]
9. Jhunjhunwala S, van Zelm MC, Peak MM, Murre C. Chromatin architecture and the generation of antigen receptor diversity. Cell. 2009; 138:435–448. [PubMed: 19665968]
10. Hewitt SL, Chaumeil J, Skok JA. Chromosome dynamics and the regulation of V(D)J recombination. Immunol Rev. 2010; 237:43–54. [PubMed: 20727028]
11. Kosak ST, Skok JA, Medina KL, Riblet R, Le Beau MM, Fisher AG, Singh H. Subnuclear compartmentalization of immunoglobulin loci during lymphocyte development. Science. 2002; 296:158–162. [PubMed: 11935030]
12. Roldán E, Fuxa M, Chong W, Martinez D, Novatchkova M, Busslinger M, Skok JA. Locus ‘decontraction’ and centromeric recruitment contribute to allelic exclusion of the immunoglobulin heavy-chain gene. Nature Immunol. 2005; 6:31–41. [PubMed: 15580273]
13. Sayegh C, Jhunjhunwala S, Riblet R, Murre C. Visualization of looping involving the immunoglobulin heavy-chain locus in developing B cells. Genes Dev. 2005; 19:322–327. [PubMed: 15687256]
14. Fitzsimmons SP, Bernstein RM, Max EF, Skok JA, Sharpiro MA. Dynamic changes in accessibility, nuclear positioning, recombination, and transcription at the Igκ locus. J Immunol. 2007; 179:5264–5273. [PubMed: 17911612]
15. Jhunjhunwala S, van Zelm MC, Peak MM, Cutchin S, Riblet R, van Dongen JJ, Grosfeld F, Knoch TA, Murre C. The 3D structure of the immunoglobulin heavy-chain locus: implications for long-range genomic interactions. Cell. 2008; 133:265–279. [PubMed: 18423198]
16. Hewitt SI, Yin D, Ji Y, Chaumeil J, Marszalek K, Tenthorey J, Salvagiotto G, Steinel N, Ramsey LB, Ghysdael J, Farrar MA, Sleckman BP, Schatz DG, Busslinger M, Bassing CH, Skok JA. RAG-1 and ATM coordinate monoallelic recombination and nuclear positioning of immunoglobulin loci. Nature Immunol. 2009; 10:655–664. [PubMed: 19448632]
17. Fuxa M, Skok J, Souabni A, Salvagiotto G, Roldan E, Busslinger M. Pax5 induces V-to-DJ rearrangements and locus contraction of the immunoglobulin heavy-chain gene. Genes Dev. 2004; 18:411–422. [PubMed: 15004008]
18. Liu H, Schmidt-Supprian M, Shi Y, Hobeika E, Barteneva N, Jumas H, Pelanda R, Reth M, Skok J, Rajewsky K, Shi Y. Yin Yang 1 is a critical regulator of B-cell development. Genes Dev. 2007; 21:1179–1189. [PubMed: 17504937]
19. Reynaud D I, Demarco A, Reddy K, Schjerven H, Bertolino E, Chen Z, Smale ST, Winandy S, Singh H. Regulation of B cell fate commitment and immunoglobulin heavy-chain gene rearrangements by Ikaros. Nature Immunol. 2008; 9:927–936. [PubMed: 18568028]
20. Hewitt SI, Farmer D, Marszalek K, Cadera E, Liang HE, Xu Y, Schlissel MS, Skok JA. Association between the lgκ and lgh immunoglobulin loci mediated by the 3′ lgκ enhancer induces ‘decontraction’ of the lgh locus in pre-B cells. Nature Immunol. 2008; 9:396–404. [PubMed: 18297074]
21. Skok JA, Brown KE, Azuara V, Caparros ML, Baxter J, Takacs K, Dillon N, Gray D, Perry RP, Merkenschlager M, Fisher AG. Nonequivalent nuclear location of immunoglobulin alleles in B lymphocytes. Nature Immunol. 2001; 2:848–853. [PubMed: 11526401]

22. Liu ZM, George-Raizen JB, Li S, Meyers KC, Chang MY, Garrard WT. Chromatin structural analyses of the mouse Igκ gene locus reveal new hypersensitive sites specifying a transcriptional silencer and enhancer. J Biol Chem. 2002; 277:32640–32649.3. [PubMed: 12080064]
23. Liu Z, Widlak P, Zou Y, Xiao F, Oh M, Li S, Chang MY, Shay JW, Garrard WT. A recombination silencer that specifies heterochromatin positioning and Ikaros association in the immunoglobulin κ locus. Immunity. 2006; 24:405–415. [PubMed: 16618599]
24. Brown KE, Guest SS, Smale ST, Hahm K, Merkenschlager M, Fisher AG. Association of transcriptionally silent genes with Ikaros complexes at centromeric heterochromatin. Cell. 1997; 91:845–854. [PubMed: 9413993]
25. Brown KE, Baxter J, Graf D, Merkenschlager M, Fisher AG. Dynamic repositioning of genes in the nucleus of lymphocytes preparing for cell division. Mol Cell. 1999; 3:207–217. [PubMed: 10078203]
26. Goldmit M, Ji Y, Skok J, Roldan E, Jung S, Cedar H, Bergman Y. Epigenetic ontogeny of the Igκ locus during B cell development. Nature Immunol. 2005; 6:198–203. [PubMed: 15619624]
27. Degner SC, Wong TP, Jankevicius G, Feeney AJ. Cutting edge: Developmental stage-specific recruitment of cohesin to CTCF sites throughout immunoglobulin loci during B lymphocyte development. J Immunol. 2009; 182:44–48. [PubMed: 19109133]
28. Kurukuti S V, Tiwari K, Tavoosidana G, Pugacheva E, Murrell A, Zhao Z, Lobanenkov V, Reik W, Ohlsson R. CTCF binding at the H19 imprinting control region mediates maternally inherited higher-order chromatin conformation to restrict enhancer access to Igf2. Proc Natl Acad Sci USA. 2006; 103:10684–10689. [PubMed: 16815976]
29. Ling JQ, Li T, Hu LF, Vu TH, Chen HL, Qui XW, Cherry AM, Hoffman AR. CTCF mediates interchromosomal colocalization between Igf2/H19 and Wbs1/Nf1. Science. 2006; 312:269–272. [PubMed: 16614224]
30. Splinter E, Heath H, Kooren J, Palstra RJ, Klous P, Grosveld F, Galjart N, de Laat W. CTCF mediates long-range chromatin looping and local histone modification in the b-globin locus. Genes Dev. 2006; 20:2349–2354. [PubMed: 16951251]
31. Yoon YS, Jeong S, Rong Q, Park KY, Chung JH, Pfeifer K. Analysis of the H19ICR insulator. Mol Cell Biol. 2007; 27:3499–3510. [PubMed: 17339341]
32. Majumder P, Gomez JA, Chadwick BP, Boss JM. The insulator factor CTCF controls MHC class II gene expression and is required for the formation of long-distance chromatin interactions. J Exp Med. 2008; 205:785–98. [PubMed: 18347100]
33. Tallquist MD, Soriano P. Epiblast-restricted Cre expression in MORE mice: A tool to distinguish embryonic vs. extra-embryonic gene function. Genesis. 2000; 26:113–115. [PubMed: 10686601]
34. Prak EL, Weigert M. Light chain replacement: A new model for antibody gene rearrangement. J Exp Med. 1995; 182:541–548. [PubMed: 7629511]
35. Coligan, JE.; Kruisbeek, AM.; Margulies, DH.; Sherach, EM.; Strober, W. Current protocols in immunology. John Wiley & Sons, Inc; New York: 1994. p. 1.9.1-1.9.3.p. 6.4.5-6.4.6.
36. Xiang Y, Garrard WT. The downstream transcriptional enhancer, Ed, positively regulates mouse Igκ gene expression and somatic hypermutation. J Immunol. 2008; 180:6725–6732. [PubMed: 18453592]
37. Inlay MA, Lin T, Gao HH, Xu Y. Critical roles of the immunoglobulin intronic enhancers in maintaining the sequential rearrangement of IgH and Igκ loci. J Exp Med. 2006; 203:1721–1732. [PubMed: 16785310]
38. Schlissel MS, Baltimore D. Activation of immunoglobulin kappa gene rearrangement correlates with induction of germline kappa gene transcription. Cell. 1989; 58:1001–1007. [PubMed: 2505932]
39. Li S, Hammer RE, George-Raizen JB, Meyers KC, Garrard WT. High level rearrangement and transcription of YAC-based mouse κ immunoglobulin transgenes containing distal regions of the contig. J Immunol. 2000; 164:812–824. [PubMed: 10623827]
40. Retter MW, Nemazee D. Receptor editing occurs frequently during normal B cell development. J Exp Med. 1998; 188:1231–1238. [PubMed: 9763602]

41. Lundgren M, Chow CM, Sabbattini P, Georgiou A, Minaee S, Dillon N. Transcription factor dosage affects changes in higher order chromatin structure associated with activation of a heterochromatic gene. Cell. 2000; 103:733–743. [PubMed: 11114330]
42. Augui S, Filion GJ, Huart S, Nora E, Guggiari M, Maresca M, Stewart AF, Heard E. Sensing X chromosome pairs before X inactivation via a novel X-pairing region of the Xic. Science. 2007; 318:1632–1636. [PubMed: 18063799]
43. Spanopoulou E, Roman CA, Corcoran LM, Schlissel MS, Silver DP, Nemazee D, Nussenzweig MC, Shinton SA, Hardy RR, Baltimore D. Functional immunoglobulin transgenes guide ordered B-cell differentiation in Rag-1-deficient mice. Genes Dev. 1994; 8:1030–1042. [PubMed: 7926785]
44. Nussenzweig MC, Shaw AC, Sinn E, Danner DB, Holmes KL, Morse HC III, Leder P. Allelic exclusion in transgenic mice that express the membrane form of immunoglobulin μ. Science. 1987; 236:816–1819. [PubMed: 3107126]
45. Wood DL, Coleclough C. Different joining region J elements of the murine κ immunoglobulin light chain locus are used at markedly different frequencies. Proc Natl Acad Sci USA. 1984; 81:4756–4760. [PubMed: 6431410]
46. Yamagami T, ten Boekel E, Andersson J, Rolink A, Melchers F. Frequencies of multiple IgL chain gene rearrangements in single normal or κL chain-deficient B lineage cells. Immunity. 1999; 11:317–327. [PubMed: 10514010]
47. Gay D, Saunders T, Camper S, Weigert M. Receptor editing:an approach by autoreactive B cells to escape tolerance. J Exp Med. 1993; 177:999–1008. [PubMed: 8459227]
48. Tiegs S, Russell DM, Nemazee D. Receptor editing in self-reactive bone marrow B cells. J Exp Med. 1993; 177:1009–1020. [PubMed: 8459201]
49. Selvakumar S, Schlissel MS. Receptor editing as a mechanism of B cell tolerance. J Immunol. 2011; 186:1301–1302. [PubMed: 21248267]
50. Schlissel MS, Schulz D, Vetterman C. A histone code for regulating V(D)J recombination. Mol Cell. 2009; 34:639–640. [PubMed: 19560416]
51. Degner-Leisso SC, Feeney AJ. Epigenetic and 3-dimensional regulation of V(D)J rearrangement of immunoglobulin genes. Semin Immunol. 2010; 22:346–352. [PubMed: 20833065]
52. Xu CR, Feeney AJ. The epigenetic profile of Ig genes is dynamically regulated during B cell differentiation and is modulated by pre-B cell receptor signaling. J Immunol. 2009; 182:1362–1369. [PubMed: 19155482]
53. Cocea L, DeSmet A, Saghatchian M, Fillatreau S, Ferradini L, Schurmans S, Weill JC, Reynaud CA. A targeted deletion of a region upstream from the Jκ cluster impairs κ chain rearrangement in cis in mice and in the 103/bcl2 cell line. J Exp Med. 1999; 189:1443–1449. [PubMed: 10224284]
54. Amin RH, Cado D, Nolla H, Huang D, Shinton SA, Zhou Y, Hardy RR, Schlissel MS. Biallelic, ubiquitous transcription from the distal germline Igκ locus promoter during B cell development. Proc Natl Acad Sci USA. 2009; 106:522–527. [PubMed: 19116268]
55. Bacher CP, Guggiari M, Brors B, Augui S, Clerc P, Avner P, Eils R, Heard E. Transient colocalization of X-inactivation centres accompanies the initiation of X inactivation. Nature Cell Biol. 2006; 8:293–299. [PubMed: 16434960]
56. Xu N, Tsai CL, Lee JT. Transient homologous chromosome pairing marks the onset of X inactivation. Science. 2006; 311:1149–1152. [PubMed: 16424298]
57. Zhao Z, Tavoosida G, Sjölinder M, Göndör A, Mariano P, Wang S, Kanduri C, Lezcano M, Sandhu KS, Singh U, Pant V, Tiwari V, Kurukuti S, Ohlsson R. Circular chromosome conformation capture (4C) uncovers extensive networks of epigenetically regulated intra- and interchromosomal interactions. Nature Genet. 2006; 38:1341–1347. [PubMed: 17033624]
58. Göndör A, Rougier C, Ohlsson R. High-resolution circular chromosome conformation capture assay. Nature Protocols. 2008; 3:303–313.
59. Cobb BS, Morales-Alcelay S, Kleiger G, Brown KE, Fisher AG, Smale ST. Targeting of Ikaros to pericentric heterochromatin by direct DNA binding. Genes Dev. 2000; 14:2146–2160. [PubMed: 10970879]
60. Su RC, Sridharan R, Smale ST. Assembly of silent chromatin during thymocyte development. Sem Immunol. 2005; 17:129–140.

61. Parelho V, Hadjur S, Spivakov M, Leleu M, Sauer S, Gregson HC, Jarmuz A, Canzonetta C, Webster Z, Nesterova T, Cobb BS, Yohomori K, Dillon N, Atagon L, Fisher AG, Merkenschlager M. Cohesins functionally associate with CTCF on mammalian chromosome arms. Cell. 2008; 132:422–433. [PubMed: 18237772]

62. Rubio ED, Reiss DJ, Welcsh PL, Disteche CM, Filippova GN, Baliga NS, Aebersold R, Ranish JA, Krumm A. CTCF physically links cohensin to chromatin. Proc Natl Acad Sci USA. 2008; 105:8309–8314. [PubMed: 18550811]

63. Stedman W, Kang H, Lin S, Kissil JL, Bartolomei MS, Lieberman PM. Cohesins localize CTCF at the KSHV latency control region and at the cellular c-myc and H19/Igf2 insulators. EMBO J. 2008; 27:654–666. [PubMed: 18219272]

64. Wendt KS, Yoshida K, Itoh T, Bando M, Koch B, Schairghuber E, Tsutsumi S, Nagae G, Ishihara K, Mishiro T, Yahata K, Imamoto F, Aburatani H, Nakao M, Imamoto N, Maeshima K, Shirahige K, Peters JM. Cohesin mediates transcriptional insulation by CCCTC-binding factor. Nature. 2008; 451:796–803. [PubMed: 18235444]

65. Hadjur S, Williams LM, Ryan NK, Cobb BS, Sexton T, Fraser P, Fisher AG, Merkenschlager M. Cohesins form chromosomal cis-interactions at the developmentally regulated IFNG locus. Nature. 2009; 460:410–413. [PubMed: 19458616]

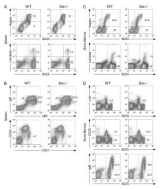

FIGURE 1.

Flow-cytometric analysis of cell surface Ig expression and B cell development in spleen and bone marrow. *A*, FACS analysis of cell surface Ig expression in WT and Sis−/− mice. Single cell suspensions from spleen were simultaneously stained with anti-B220 and anti-Igκ antibodies (upper); or anti-B220 and anti-Igλ antibodies (lower). Stained cells were analyzed by FACS. Only cells residing in the lymphocyte gate were analyzed. Percentages of cells residing in various windows are shown in the figure sub-panels. Data are representative of independent FACS analyses from at least 6 mice of each genotype. *B*, FACS analysis of transitional, follicular mature, and marginal zone B cells in WT and Sis−/− mice. Single cell suspensions from spleen were simultaneously stained with anti-IgM and anti-IgD antibodies (upper); or anti-CD21 and anti-CD23 antibodies (lower). *C*, FACS analysis of cell surface Ig expression in bone marrow of WT and Sis−/− mice. Single cell suspensions from bone marrow were stained and analyzed as described in *A*. Only cells residing in the lymphocyte gate were analyzed. Data are representative of independent FACS analyses from at least 6 mice of each genotype. *D*, FACS analysis of B cell development in bone marrow of WT and Sis−/− mice. Single cell suspensions from bone marrow were stained with anti-B220 and anti-c-kit antibodies to assay for pro-B cells (upper), anti-B220 and anti-CD25 antibodies to assay for pre-B cells (middle), or anti-B220 and anti-IgM to assay for immature and mature B cells (lower).

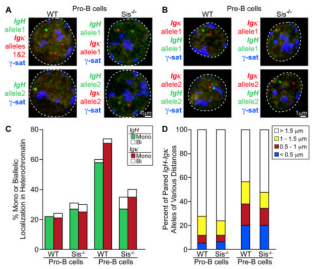

FIGURE 2.

Three-color 3D DNA FISH for localization of *Igκ*, *IgH* and γ-satellite sequences in pro- and pre-B cell nuclei from WT and Sis−/− mice. *A* and *B*, Representative confocal 0.3 μm-thick optical sections of probe hybridization patterns in single nuclei of bone marrow derived pro- and pre-B cells from WT and Sis−/− mice as indicated. The two *Igκ* and two *IgH* alleles in each cell can be viewed in the separate optical sections that are shown (upper and lower subpanels). BAC probes used were complementary to Vh *IgH* (green) and to Vκ *Igκ* (red) sequences, and a plasmid probe complementary to γ-satellite sequences (blue). Nuclei are outlined by white dashed lines as identified by DAPI staining and allele hybridization patterns are indicated in the left hand margins. *C*, Histograms representing the % mono- or biallelic localization in pericentromeric heterochromatin domains of *IgH* (green) and *Igκ* (red) sequences in pro- and pre-B cells of WT and Sis−/− mice as indicated. For each specimen 100 nuclei were scored. Similar results were obtained in several additional independent experiments (Supplementary Table S2*A*,*B*,*C*,*D*). *D*, Histograms representing the percentages of paired *IgH*-*Igκ* alleles of various distances (color-coded key) in pro- and pre-B cells of WT and Sis−/− mice as indicated. For each specimen 80 nuclei were scored. Similar results were obtained in an additional independent experiment (Supplementary Table S2*E*).

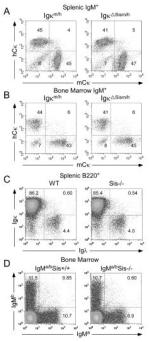

FIGURE 3.

Analysis of *Igκ* and *IgH* allelic exclusion, and *IgL* isotype exclusion. *A and B,* Analysis of *Igκ* allelic exclusion. Single cell suspensions from spleen (*A*) and bone marrow (*B*) were simultaneously stained with anti-B220, anti-mouse-Igκ (mCκ), anti-human-Igκ (hCκ) and anti-IgM antibodies. The expression of mCκ and hCκ in $Ig\kappa^{m/h}$ and $Ig\kappa^{\Delta sism/h}$ mice splenic (*A*) or bone marrow (*B*) $B220^{+}IgM^{+}$ cells were analyzed by FACS. Percentages of cells residing in various windows are shown in the figure sub-panels. Data are representative of independent FACS analyses from at least 6 mice of each genotype. *C,* Analysis of *Igκ* and *Igλ* isotype exclusion. Single cell suspensions from spleen were simultaneously stained with anti-B220, anti-Igκ and anti-Igλ antibodies. The expression of Igκ and Igλ in WT and Sis−/− mice splenic $B220^{+}$ cells were analyzed by FACS. Data are representative of independent FACS analyses from at least 5 mice of each genotype. *D,* Analysis of *IgH* allelic exclusion. Single cell suspensions from bone marrow were simultaneously stained with anti-IgM^{a} and anti-IgM^{b} antibodies. The expression of IgM^{a} and IgM^{b} cells in bone marrow were analyzed by FACS. Data are representative of independent FACS analyses from at least 4 mice of each genotype.

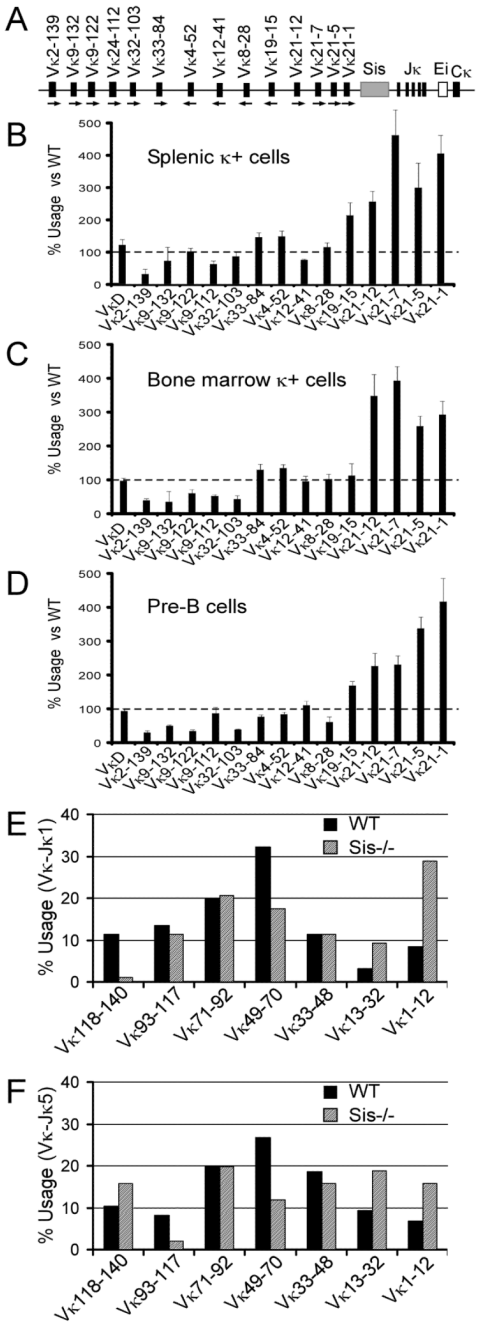

FIGURE 4.

Vκ gene repertoire analysis in B cells. *A*, Diagram of the relative positions and orientations (lower arrows) of specific Vκ genes assayed for their rearrangement status in the locus (not to scale). Vκn specific primers and a primer downstream of Jκ1r were used to assay for specific Vκ-Jκ1 rearrangements in genomic DNA by real-time PCR. *B–D*, Usage of different Vκ genes in κ+ cells from spleen and bone marrow (*B & C*) and pre-B (*D*) cells. The % usage of Vκ genes in Sis−/− mice was compared with those of WT mice in which the % usage was set as 100% (depicted as dashed lines). *E*, The Vκ-Jκ1 rearrangement products of pre-B cells from WT and Sis−/− were amplified from genomic DNA by PCR and sub-cloned into the PGEM-T vector. Approximately 100 independently determined Vκ gene

sequences from each group were identified by IgBlast. The usages of the indicated groups of Vκ gene sequences in WT and Sis−/− cells are shown. *F*, The Vκ-Jκ5 rearrangement products of pre-B cells from WT and Sis−/− were similarly identified as above.

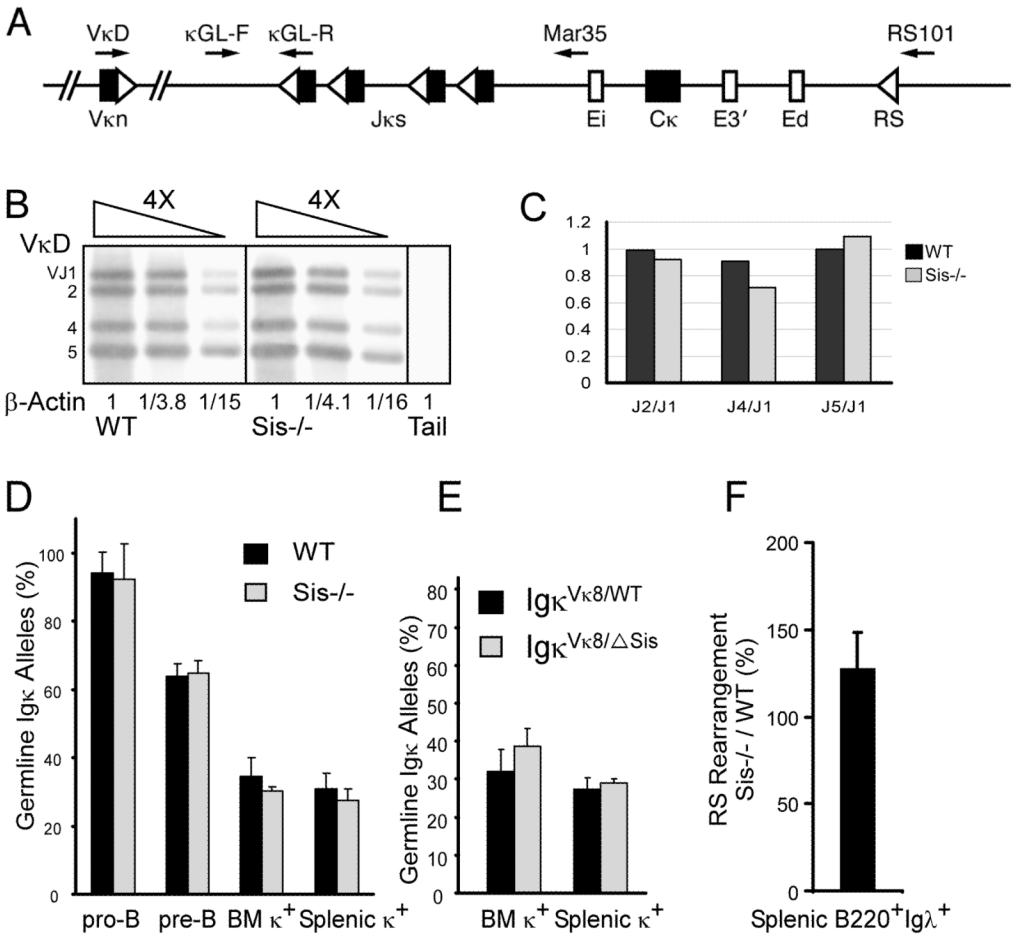

FIGURE 5.

Analysis of Jκ usage, *Igκ* gene germline levels and RS rearrangement in WT and Sis−/− B cell populations. *A*, The schematic depicts the positions in the Igκ locus (not to scale) of the degenerate VκD primer and other indicated primers used in various PCR assays (arrows). Vκ, Jκ, and Cκ exons are closed rectangles, Ei, E3′, and Ed enhancers are open rectangles, and RSS or RS elements are open triangles. *B*, VκD and Mar35 primers were used to amplify Vκ-Jκ rearrangements from splenic Igκ$^+$ cells' genomic DNA. Vκ-Jκ rearrangement PCR products were separated by electrophoresis on agarose gels and the intensities of Vκ-Jκ1 to Vκ-Jκ5 bands were quantitated by PhosphorImager analysis of Southern blot results. The real-time PCR results of β-actin amplification are shown at the bottom, which were used as genomic DNA template controls in the PCR reactions. *C*, The relative usage of the indicated Jκ regions are shown as ratios for WT and Sis−/− Igκ$^+$ cells are shown. *D*, The κGL-R primer is complementary to the Jκ1 intronic region, and the κGL-F is complementary to a region upstream of the Jκ1 RSS sequence that will be deleted after Vκ-Jκ rearrangement. Real-time PCR analysis of the percentage of germline Igκ alleles (κGL) in the indicted B cell populations from WT and Sis−/− mice. κGL levels were normalized to the levels of a β-actin genomic region and theκGL level in ES cells was set as 100%. Each sample represents tissue pools from 2–4 mice of the same genotype and all experiments were repeated at least two independent times. *E*, Real-time PCR analysis of the percentage of germline *Igκ* alleles in *Igκ*$^{Vκ8/WT}$ and *Igκ*$^{Vκ8/ΔSis}$ mice. *F*, Real-time PCR assay analysis of the levels of RS rearrangement in splenic Igλ+ B cells using the VκD and RS101 primers. RS rearrangement levels were normalized to the levels of a β-actin genomic region and the

RS rearrangement level in WT splenic $B220^{+}Ig\lambda^{+}$ cells was set as 100%. Data are presented as means ± SD (n = 3). Each sample represents tissue pools from 2 mice of the same genotype.

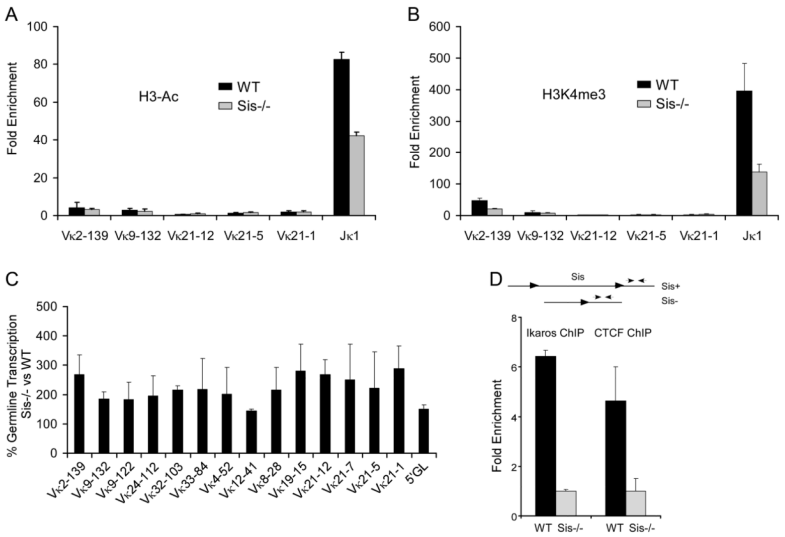

FIGURE 6.

Assay of signatures of chromatin accessibility and silencing in the *Igκ* locus in pre-B cells from WT and Sis−/− mice. *A.* Real time PCR ChIP assays of H3-Ac levels in pre-B cells of WT and Sis−/− mice as indicated for specific Vκ genes and the Jκ1 region. Fold enrichment refers to the sequence abundance in the immunoprecipitated sample divided by the corresponding sequence abundance in input DNA relative to a control α-actin gene sequence. Data are presented as means ± SD (n=3). *B.* Real time PCR ChIP assays of H3K4me3 levels in pre-B cells of WT and Sis−/− mice as in panel *A*. Data are presented as means ± SD (n=3). *C.* The results of real-time PCR assays used to measure Igκ gene germline transcription in pre-B cells initiated from the 5′ promoter (5′GL) and the indicated specific Vκ genes from WT and Sis−/− mice. Data are presented as means ± SD (n=3). *D.* IKAROS and CTCF ChIP assays of pre-B cell chromatin from WT and Sis−/− mice. In the upper segment of the schematic map, the Sis element is depicted with flanking loxP sites (arrowheads) before its deletion by *Cre* recombinase. PCR primers residing 3′ of Sis complementary to sequences common between Sis+ and Sis- alleles are also shown (small arrowheads). Real-time PCR ChIP assays of IKAROS and CTCF occupancy are shown for WT and Sis−/− samples. Results represent mean ± SD of two independent ChIP experiments.

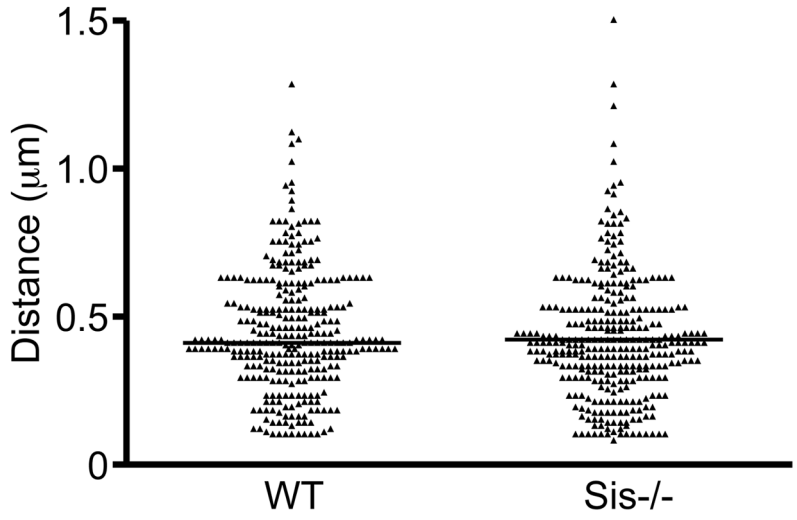

FIGURE 7.

Two-Color 3D FISH for assessment of contraction of the *Igκ* locus in pre-B cell nuclei from WT and Sis−/− mice. The scatter plots depict pair-wise distance measurements between the centers of hybridizing signals from BAC probes at 5′ and 3′ locations in the locus. Data from 311 WT and 323 Sis−/− pre-B cell alleles accumulated from measurements in several independent experiments. Median values are indicated by horizontal lines, which are not significantly different ($P>0.5$). Similar results were obtained in several other independent experiments and also no significant differences were noted for WT vs Sis−/− pro-B cells for contraction of the *Igκ* locus nor for *IgH* locus contraction in similar samples (Supplemental Table S2*F*,*G*).